Proceedings of the ASME 2018
International Mechanical Engineering Congress and Exposition
IMECE2018
November 9-15, 2018, Pittsburgh, PA, USA

IMECE2018-88107

MULTI-SCALE MODELING OF POWER PLANT PERFORMANCE ENHANCEMENT USING ASYNCHRONOUS THERMAL STORAGE AND HEAT REJECTION

Lauren B. Gagnon, Dre Helmns, and Van P. Carey
Department of Mechanical Engineering
University of California Berkeley
Berkeley, California, USA

ABSTRACT

The study summarized in this paper links a model of thermal energy storage (TES) unit performance to a subsystem model including heat exchangers that cool down the storage at night when air temperatures are low; this cool storage is subsequently used to precool the air flow for a power plant air-cooled condenser during peak daytime air temperatures. The subsystem model is also computationally linked to a model of Rankine cycle power plant performance to predict how much additional power the plant could generate as a result of the asynchronous cooling augmentation provided by this subsystem. The goal of this study is to use this model to explore the parametric effects of changing phase change material (PCM), melt temperature, and the energy input and rejection control settings for the system. With this multi-scale modeling, the performance of the TES unit was examined within the context of a larger subsystem to illustrate how a high efficiency, optimized design target can be established for specified operating conditions that correspond to a variety of applications. Operating conditions of interest are the mass flow rate of fluid through the flow passages within the TES, the volume of the TES, and the amount of time the system remains in the extraction process in which thermal energy is inputted to the device by melting PCM, and the PCM melt temperature. These conditions were varied to find combinations that maximized efficiency for a 50 MW power plant operating in the desert regions of Nevada during an average summer day. By adjusting the flow rate within the fluid flow passages and the volume of the TES to achieve complete melting of the PCM during a set extraction time, indications of the parametric effects of system flow, melt temperature, and control parameters were obtained. The results suggest that for a full-sized power plant with a nominal capacity of 50 MW, the kWh output of the plant can be increased by up to 3.25% during the heat input/cold extraction period, depending on parameter choices. Peak power output enhancements were observed to occur when the system operated in the extraction phase during limited hours near the peak temperatures experienced throughout a day, while total kWh enhancement was shown to increase as the extraction period increased. For the most optimized conditions, cost analyses were performed, and it was estimated that the TES system has the potential to provide additional revenue of up to $1,366 per day, depending on parameter choices as well as the local cost of electricity. Results obtained to date are not fully optimized, and the results suggest that with further adjustments in system parameters, weather data input, and control strategies, the predicted enhancement of the power output can be increased above the results in the initial performance predictions reported here.

NOMENCLATURE

ε_{hx}	Effectiveness of external heat exchanger (HX); may be written as ε_{source} or ε_{sink}
$\dot{Q}$	Heat transfer rate in the external HX
ρ_w	Working fluid density
c_{pw}	Working fluid specific heat
h_{ls}	Latent heat of fusion of PCM
$\bar{\rho}_e$	Effective density of TES differential element
$\bar{c}_{pe}$	Effective specific heat of differential element
s_w	Wetted perimeter of flow passage
A_c	Cross sectional area of flow passage
v'	PCM matrix volume per unit flow length
T_m	Melting temperature of PCM
T_e	TES device matrix element temperature
T_w	TES device working fluid temperature
T_{open}	External HX open loop working fluid temperature; may be written as T_{source} or T_{sink}
T_{closed}	TES closed loop working fluid temperature; may be written as T_{ext} or T_{char}
U	Overall heat transfer coefficient between bulk working fluid and PCM matrix element
$\dot{m}_{closed}$	Working fluid closed loop mass flow rate through TES; may be written as $\dot{m}_{ext}$ or $\dot{m}_{char}$

$\dot{m}_{open}$ Working fluid open loop mass flow rate through external HX; may be written as $\dot{m}_{source}$ or $\dot{m}_{sink}$
C_{min} Minimum heat capacity rate in external HX
t_{ext} Time elapsed to end of extraction process
x_e Melt Fraction of PCM in matrix element
$\eta_{rankine}$ Efficiency of power plant Rankine cycle
$\dot{W}$ Power produced resulting from precooling by external HX

INTRODUCTION

This paper links a model of thermal energy storage (TES) unit performance to a subsystem model including heat exchangers that cool down the storage at night when air temperatures are low, and precool the air flow for a power plant air-cooled condenser during peak daytime air temperatures. The subsystem model was also computationally linked to a model of Rankine cycle power plant performance to predict how much additional power the plant could generate as a result of the asynchronous cooling augmentation provided by this subsystem.

Earlier analyses of phase change thermal storage performance have generally modeled specific details of heat transfer in the storage unit structure with constant boundary conditions, thereby neglecting interaction within a subsystem. For example, M. M. Alkilani et. al [1] conducted a theoretical investigation of output air temperature of an indoor heater which utilizes a PCM heat exchanger. In this model, the PCM was used to store solar heat from throughout the day. After the sun set and cooler temperatures were experienced indoors, the cooler ambient air from inside could be directed through the PCM heat exchanger to warm up and flow back into the room to provide heating. This model implemented only a constant input air temperature to the PCM heat exchanger, which was provided by the ambient air temperature from inside the room desired to be heated, thereby neglecting the inevitable changes in the room's, and therefore input air's, temperature. Of the few analyses that have considered a variable inlet air temperature, such as the one produced by S. M. Vakilaltojjar and W. Saman [2], a simple system consisting only of a PCM heat exchanger was examined, whereas the system considered in this paper includes an external heat exchanger which governs the temperature of the working fluid within the PCM heat exchanger.

This paper builds upon previous work by Helmns and Carey to model a 24-hour cycle operation of a TES subsystem connected to a Rankine cycle power plant [3]. Helmns and Carey's model, however, does not incorporate real-world temperature data as this one does. Furthermore, their work does not explore optimization of the TES subsystem nor the financial payback period associated with use of such technology, whereas such analyses are performed and explained in detail here.

The method of quantifying effectiveness used in the modeling techniques utilized by this paper are not significantly different from prior work, but the analysis of a TES device with temporally transient boundary conditions and spatially varying inlet conditions in a multi-scale modeling approach, depicted in Figure 1, is novel and facilitates exploring a subsystem that models realistic operating conditions for a TES.

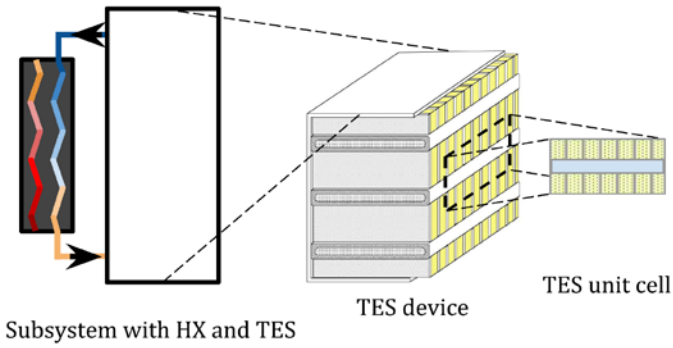

Fig. 1. Schematic depicting multi-scale nature of problem ranging from the subsystem including the external heat exchanger to the TES device to the unit cell differential element (containing fins, PCM, and flow passage)

The motivation behind the described modeling is the high usage of water at power plants. Traditionally, steam produced by thermo-electric power plants is cooled by directing it over an array of pipes filled with cold water, which causes the steam to condense. This process is highly water intensive and uses between 730 and 830 gal/MWh [4]. Not only is this cooling method impractical in areas where water conservation is an issue, but it also causes irreparable damage to many rivers and reservoirs. To replace this process with a more sustainable one, research is currently being conducted to show proof of concept air cooling technology using TES in conjunction with a PCM that could potentially reduce water usage at power plants. However, there is no plan in place to make this technology a reality in full scale power plants. If this technology could be implemented into power plants worldwide, it could make a dramatic impact on water conservation efforts and facilitate the restoration of water sources for cities around the world.

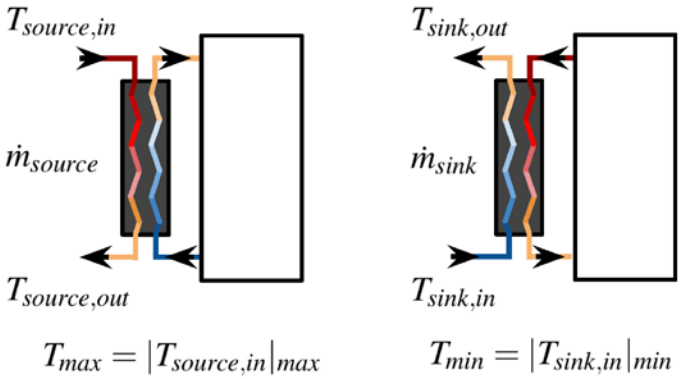

Fig. 2. TES coupled with an external heat exchanger for cold extraction (left) and cold charging (right)

The proposed TES device that is exhibited in the model utilized by this paper operates in the following way. The TES device can be used to gather energy during the day, store it, and then reject it asynchronously (at night) rather than continuously throughout the day as is standard in many applications. This is particularly useful for many reasons. First, asynchronous cooling removes the need for peak load production, which is

typically more expensive both financially and environmentally. Second, temperature differences are greater at night when ambient air is cooler, rendering heat transfer more thermodynamically efficient from a simple Carnot standpoint. The type of cold storage considered here can be used for asynchronous cooling in a number of applications including rural refrigeration, building air conditioning, and steam power plants.

Figure 2 depicts a thermal energy storage device paired with an external heat exchanger, one connected in open loop to a heat source, and the other to a heat sink. A thermal energy storage device is connected via a closed loop that circulates through the heat exchanger.

To visualize how this works, a full-scale schematic is depicted in Figure 3, and a simple cycle that can be used to cool the steam condenser in a power plant can be considered. Ideally, it is preferable to begin with a completely frozen device. To achieve this, a cold working fluid ($\dot{m}_{sink} > 0$) is sent from a sink ($T_{sink,in}$) through the heat exchanger to cool a counterflowing fluid entering the thermal energy storage unit. Provided that the temperature of the fluid entering the TES device is less than the melt temperature, T_m, the PCM will undergo freezing, as shown in Figure 3.3. Next, a quiescent storage period would take place, as shown in Figure 3.4. During storage, no flow occurs in the system ($\dot{m}_{closed} = 0$). These periods are strategically designed to occur when the inlet air temperature is very close to the melting temperature of the PCM ($T_m \pm 0.8$°C), as little to no advantage would be gained from running the TES system during this time. If desired, the bypass door could be opened throughout storage to allow air directly from the surrounding environment to cool the steam condenser. After storage, a hot working fluid ($\dot{m}_{source} > 0$) from a source ($T_{source,in}$) can be chilled by sending it through the heat exchanger, delivering heat to the closed loop fluid entering the thermal storage unit. This warm working fluid will reject heat to the cold storage matrix, provided its temperature is greater than T_m, thereby melting the PCM and chilling the closed-loop working fluid. This will chill the open-loop working fluid ($T_{source,out}$) which can be used to augment cooling in various applications, as shown in Figure 3.1. After a second quiescent storage period, as shown in Figure 3.2, the cycle would begin again.

With the described subsystem, the heat exchanger could be connected to a Rankine cycle or air conditioning condenser in order to precool the open loop fluid and reduce the temperature at which steam or another refrigerant is condensed. At a later time, when the temperature difference with ambient is more favorable, the energy collected from precooling could be released as heat via the same heat exchanger. In short, the idea is to use cold storage to decrease the low system temperature of the power or refrigeration cycle by heat rejection load shifting without burning fuel or wasting water.

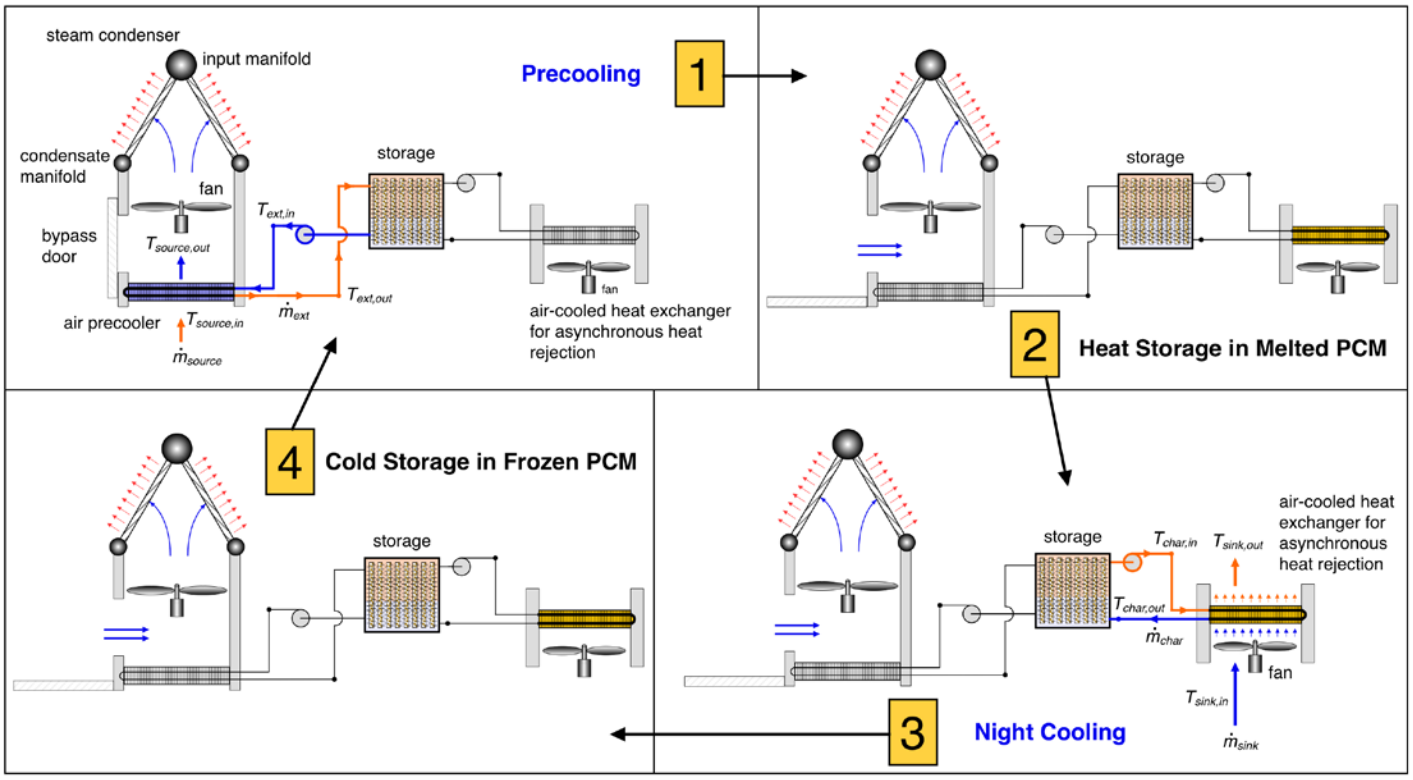

Fig. 3. Case study cycle consisting of precooling, storage, night cooling, and storage once more

MODEL

The model utilized by this paper was developed by Helmns and Carey [3]. Helmns and Carey's model is similar to that of a compact heat exchanger; however, it considers a transient process in which a PCM either stores or rejects heat through latent heat transfer while a phase change is occurring. In this model, it is assumed that the working fluid in the TES unit either flows through a single passage or the flow is manifolded to multiple identical passages. Turns are ignored, and instead, the focus of Helmns and Carey's analysis is on a unit cell of one long passage, with the mass flow rate per passage designated as $\dot{m}_{closed}$. The unit cell, of length *dz*, is composed of the working fluid flow passage and the surrounding PCM section. This element includes the tube wall and fin structures that conduct heat into the PCM. To derive the governing equations, a control volume is used, with one control volume around a differential element of PCM matrix and another around a differential section of the flow passage. Conservation of energy is applied to each of these control volumes, noting that the stored thermal energy must be balanced by the thermal energy transport across the control surfaces of each unit cell. From the definition of enthalpy for a solid-liquid mixture, thermal energy in the PCM matrix can be stored in sensible and latent forms, as shown in the following differential equations in Equations (1) and (2).

For $T_e \neq T_m \; and \; x_e = 0 \; or \; x_e = 1$:

$$\frac{\partial T_e}{\partial t} = \frac{U s_w}{\bar{\rho}_e \bar{c}_{pe} v'} (T_w - T_e); \; \frac{\partial x_e}{\partial t} = 0 \tag{1}$$

Equation (1) represents the transient exchange of sensible energy between the working fluid and the PCM. This energy input or rejection is accompanied by changing temperature within the storage element.

For $T_e = T_m$ and $0 < x_e < 1$:

$$\frac{\partial x_e}{\partial t} = \frac{U s_w}{\bar{\rho}_e h_{ls} v'} (T_w - T_e); \; \frac{\partial T_e}{\partial t} = 0 \tag{2}$$

When a storage element reaches the melt temperature, phase change occurs. Equation (2) dictates the transient exchange of latent energy between the working fluid and the PCM that leads to melting or freezing.

Likewise, conservation of energy on a control volume around the working fluid (inside the flow passage) of the unit cell requires that stored energy must be balanced by advection as well as heat transfer to and from the PCM matrix, as shown in the differential equation in Equation (3).

$$\frac{\partial T_w}{\partial t} = -\left(\frac{\dot{m}_{closed}}{\rho_w A_c}\right) \frac{\partial T_w}{\partial z} + \frac{U s_w}{\rho_w A_c c_{pw}} (T_e - T_w) \tag{3}$$

To account for the energy exchange across the flow channel wall, an additional equation for the working fluid temperature is required. Equation (3) describes that energy is advected along the working fluid channel as well as exchanged with the storage element throughout the passage.

Equations (1) through (3) are subsequently non-dimensionalized and solved, rendering them scalable for any application. The results from these equations are then dimensionalized once more to generate meaningful information for the system. As the focus of this paper is on the impact of TES for power plants, only the dimensional results will be discussed. Further, highly detailed information on the dimensionless framework can be found in prior work [3].

These energy balances neglect conduction in the downstream direction. It can be shown that the ratio of stream-wise conduction to transport to or from the PCM is small for TES designs of interest. In other words, the heat diffusion effect is small compared to convection and conduction normal to the flow passage walls for the configuration considered in Helmns and Carey's model. These coupled equations are first order in time and space, necessitating initial conditions for temperatures and melt fraction as well as an inlet boundary condition for the working fluid temperature.

Building off the differential equations depicted in Equations (1) through (3), the subsequent equations that are implemented in Helmns and Carey's model produce the results of interest in this paper. While Equations (4) through (7) are not again derived here, general explanations of the equations are described.

$$T_{ext,in} = T_{source,in} - \frac{\dot{Q}_{source}}{C_{min} \varepsilon_{source}} \tag{4}$$

$$T_{ext,out} = \varepsilon_{so} \frac{C_{min}}{(\dot{m} c_p)_{ext}} T_{so,in} + \left(1 - \varepsilon_{so} \frac{C_{min}}{(\dot{m} c_p)_{ext}}\right) T_{ext,in} \tag{5}$$

$$T_{char,in} = \frac{\dot{Q}_{sink}}{\varepsilon_{sink} C_{min}} + T_{sink,in} \tag{6}$$

$$T_{ch,out} = \varepsilon_{si} \frac{C_{min}}{(\dot{m} c_p)_{ch}} T_{si,in} + \left(1 - \varepsilon_{si} \frac{C_{min}}{(\dot{m} c_p)_{ch}}\right) T_{ch,in} \tag{7}$$

Equation (4) is the performance equation for the precooler. Equation (5) is an expression that solves for the inlet working fluid temperature to the TES during extraction which is derived from performance and conservation equations. Equation (6) is the performance equation for the night cooler, and Equation (7) is an expression that solves for the inlet working fluid temperature to the TES during charging, which is derived from performance and conservation equations. In summary, Equations (4) through (7) are used to calculate the input and output air temperatures from both the precooler and the night cooler. It should also be noted that Equation (2) is used to calculate the melt fraction of the PCM.

Table. 1. TES case study dimensional variables – geometry

Wetted perimeter of flow passage, s_w	0.0471	m
Length of flow passage, *L*	0.407	m
Cross sectional area of flow passage, A_c	0.0000449	m^2
PCM matrix volume per unit flow length, *v'*	0.0000996	m^2

Finally, it should be discussed that the PCM utilized in this analysis by the described model is Lithium Nitrate TriHydrate ($LiNO_3$,$3H_2O$). This material is a reliable salt hydrate with almost no subcooling effect or observed phase segregation during thermocycling in tests involving small mass and large mass samples. The only potential setback is the cost compared to other inorganic PCM options; however, based on volumetric storage ability, Lithium Nitrate TriHydrate is one of the best PCMs to consider. Some important properties of this material are its melting/freezing temperature of 30°C and its latent heat of

fusion of 278.14 kJ/kg. The volume of the TES, used as a metric in this paper, is calculated by finding the required number of flow channels to determine the total frontal area ($n_{chan} * A_c + (n_{chan} - 1) * v'$) and multiplying that quantity by the length of the flow passage (L). This volume includes both the PCM matrix and the flow passages in the TES, with geometry in Table 1.

RESULTS

To explore a subsystem that models realistic operating conditions for a TES, a moderate plant size of 50 MW and a PCM melt temperature of 30°C (the melting temperature of Lithium Nitrate TriHydrate) were chosen as a starting point to model. A specific water-scarce location with need to utilize water conservation techniques was also selected to provide an area in which the TES would be beneficial. In this case, Las Vegas, Nevada is the chosen location because it lies in a desert region less than 50 miles away from the Walter Higgins Generating Station, a powerplant that currently utilizes air cooling techniques and could benefit from the TES precooling system discussed in this paper.

With Las Vegas chosen as the region of interest, and the modeling techniques determined, hourly weather data from January 2013 through December 2017 was obtained from the Las Vegas Henderson Airport Weather Station (WBAN 53127) through use of the Local Climatological Data Tool on the NOAA website [5]. Because the precooling process is most necessary when the outside air temperature is hottest, July and August were selected as the months that would be further analyzed. The hourly temperature data from 2013 to 2017 for July and August are plotted in Figures 4 and 5, respectively. Looking at the average hourly temperatures over the years, it can be seen that July has a peak temperature of nearly 37°C, and August has a peak temperature of nearly 35°C.

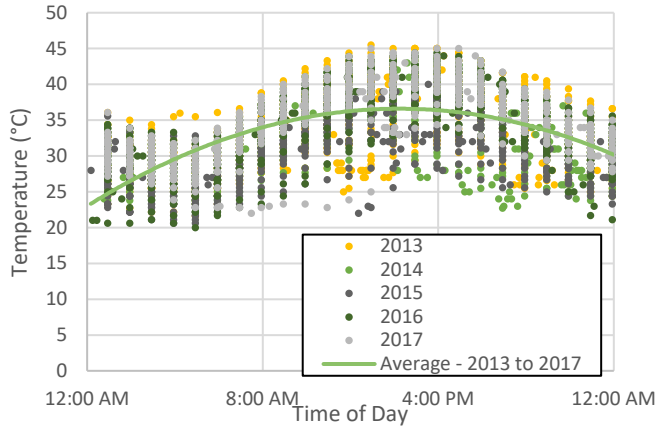

Fig. 4. Hourly temperature data for the month of July in Las Vegas, NV for 2013 to 2017

These peak temperatures put the month of July as the best candidate to analyze for the precooling process for the purposes of this paper. However, another factor to consider is also the minimum temperature achieved throughout the day and how that relates to the selected PCM melt temperature of 30°C. There is a concern that the ambient nighttime temperature might not dip below the melt temperature of the PCM, which would impede recharging of the TES device. Therefore, environments that are more likely to reach sufficiently low temperatures at night are selected for analysis in this paper. In practice, the TES would include a control system to regulate its operation based on daily weather data and future weather predictions. Such a control system would be able to manage which days it would be optimal to have the TES in use.

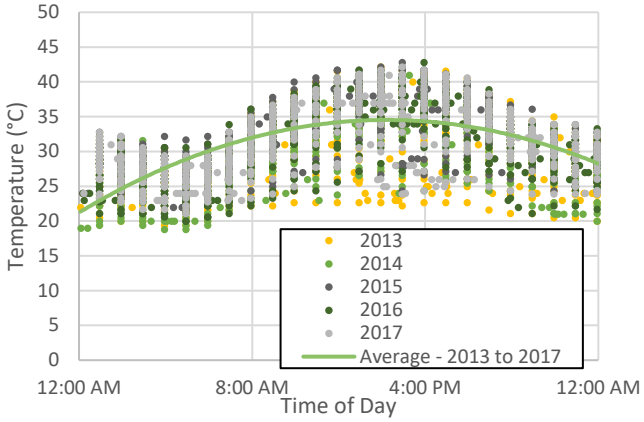

Fig. 5. Hourly temperature data for the month of August in Las Vegas, NV for 2013 to 2017

Figures 6 and 7 show the average hourly temperature curves of days in July and August, respectively. Reviewing these two figures, it was observed that the average daily minimum temperature in July is only about 3°C below the PCM melt temperature, but the average daily minimum temperature in August is about 6°C below the PCM melt temperature. Therefore, August was selected as the month to analyze in the model for the precooling process.

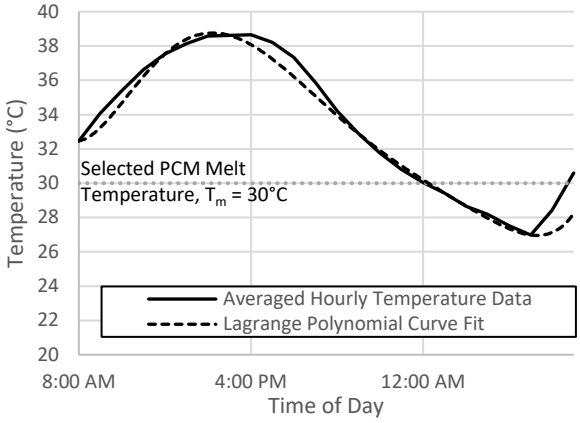

Fig. 6. Hourly Las Vegas, NV temperature data for July averaged from 2013 to 2017

Inputting the average hourly temperatures for the month of August into the model, an approximate temperature curve for an average 24-hour period in August was generated using a polynomial fit, as shown in Figure 8. Reviewing this

temperature curve, it was determined that, based on the selected PCM melt temperature of 30°C, extraction could be implemented for a maximum of 12 hours. Using this extraction time as a starting point, the model was adjusted to contain a PCM that was large enough to be fully utilized throughout the entire extraction period, and the flow rate per channel in the PCM was adjusted such that the extraction and charging processes would both reach 95% effectiveness, which corresponds to 95% of the PCM's mass melting and freezing, respectively.

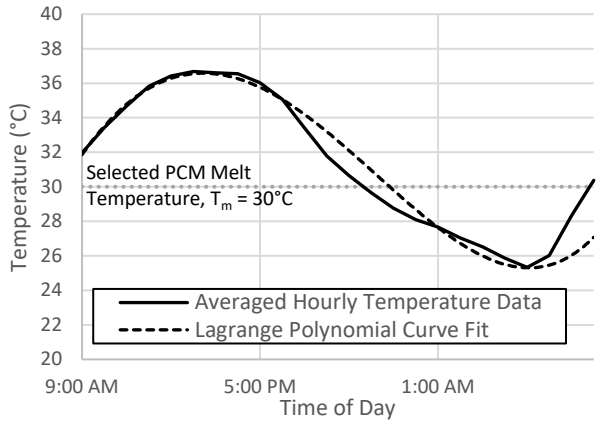

Fig. 7. Hourly Las Vegas, NV temperature data for August averaged from 2013 to 2017

After adjusting parameters, the August temperature curve was inputted into the model. The results from using this ambient temperature data, the chosen PCM melt temperature, and the selected amount of PCM can be seen in Figure 9. In this plot, the melt fraction curve shows that the PCM was nearly fully melted and refrozen throughout the day. Figure 9 also shows that during extraction, the precooling process decreases the air inlet temperature into the steam condenser by about 6°C, which greatly improves the ability of the plant to efficiently generate energy.

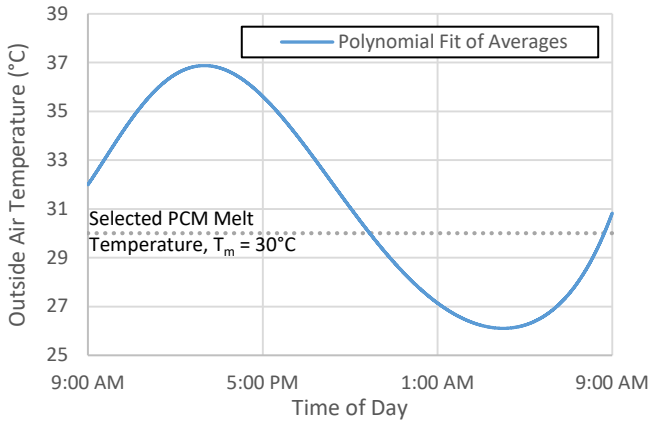

Fig. 8. Outside air temperature throughout an average August day in Las Vegas, NV

In fact, the gains achieved through this decrease in air temperature over the 12-hour extraction period can be calculated by using the following equations. First, the efficiency of the Rankine cycle of the power plant is calculated,

$$\eta_{rankine} = 0.6\left(1 - \frac{T_{source,out}}{T_{boiler}}\right) \quad (8)$$

where T_{boiler} is the boiler temperature, which in this case was set to 362.4°C. Next the power output is calculated,

$$\dot{W} = \dot{Q}\left(\frac{\eta_{rankine}}{1-\eta_{rankine}}\right) \quad (9)$$

Subsequently, the energy produced over the extraction period is calculated.

$$E_{ext} = \int_0^{t_{ext}} \dot{W}\, dt \quad (10)$$

Next, the energy produced over the day, E_{day}, is calculated.

$$E_{day} = \int_0^{24\ hrs} \dot{W}\, dt \quad (11)$$

Following these calculations, the gain in energy over the extraction period, ΔE_{ext}, is calculated,

$$\Delta E_{ext} = E_{ext} - E_{no\ ext} \quad (12)$$

where $E_{no\ ext}$ is the energy produced over the extraction period but as if the extraction process had not taken place, so there was no precooling effect. Finally, the percent gain in energy production over the extraction period, $\%\uparrow E_{ext}$, and the percent gain in energy production over the day, $\%\uparrow E_{day}$, are calculated.

$$\%\uparrow E_{ext} = \frac{\Delta E_{ext}}{E_{no\ ext}} \quad (13)$$

$$\%\uparrow E_{day} = \frac{\Delta E_{ext}}{E_{no\ ext} + E_{day}} \quad (14)$$

Using Equation (13), it is found that the 6°C temperature difference seen in Figure 9 increases the kWh produced during the extraction period by 1.70%, and using Equation (14), it is calculated that the temperature difference increases the kWh produced throughout the entire day by 0.85%. These percentages correspond to a production gain of 10.4 MWh, as calculated with Equation (10).

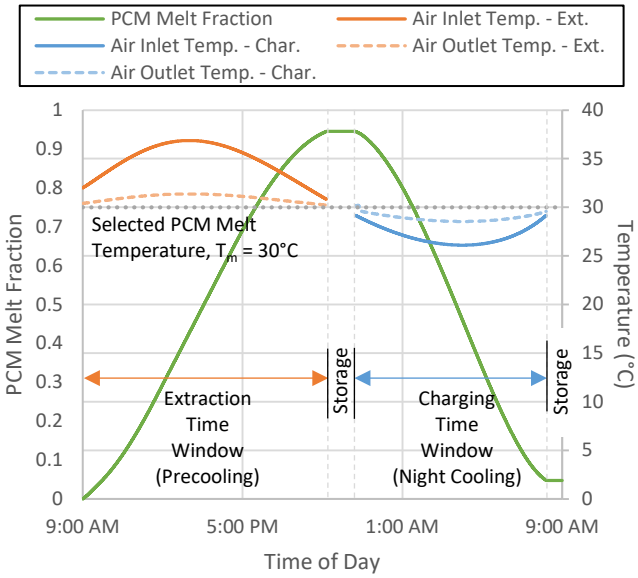

Fig. 9. Melt fraction of PCM and air inlet and outlet temperatures to and from TES for extraction (12 hours) and charging vs. time of day in Las Vegas, NV for average day in August

While this is a substantial amount of energy gain, the goal of the precooling process is to increase the efficiency of energy production by as wide a margin as possible. With this goal in mind, it was decided to test several different extraction periods to see if energy production could be further increased. To ensure that the PCM was being fully utilized throughout these extraction periods, the number of channels in the PCM as well as the flow rate per channel in the PCM were adjusted such that the extraction and charging processes would reach 95% effectiveness. Figure 10 shows the relationship between the percent increase in kWh over the extraction period and the volume of the TES. This data shows a very clear relationship in which the percent kWh gained over the extraction period increases as the volume of the TES, and therefore the length of extraction, increases.

Figure 11 shows the relationship between the percent increase in kWh over the extraction period and the volume of the TES. This data shows a relationship in which the percent kWh gained over the extraction period decreases as the volume of the TES, and therefore the length of extraction, increases.

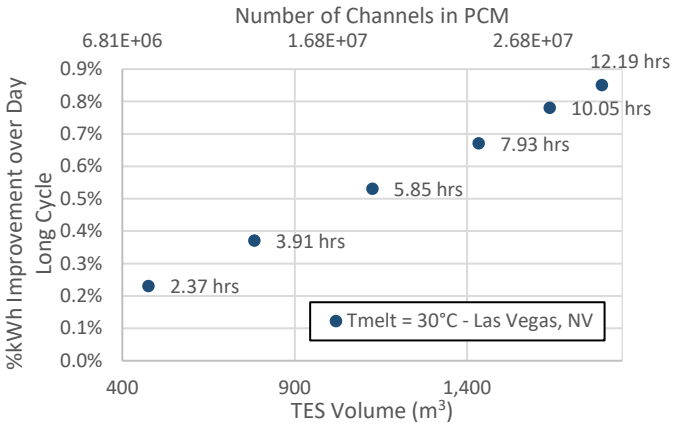

Fig. 10. %kWh gained over day for different lengths of extraction periods vs. TES volume for PCM melting temperature of T_m = 30°C in Las Vegas, NV for average day in August

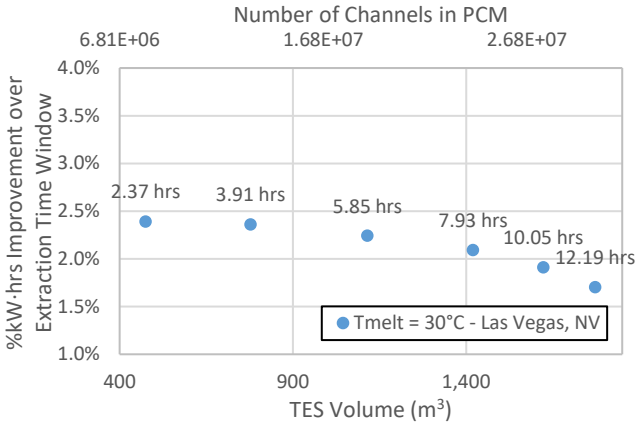

Fig. 11. %kWh gained over extraction time for different lengths of extraction periods vs. TES volume for PCM melting temperature of T_m = 30°C in Las Vegas, NV for average day in August

The two relationships in Figures 10 and 11 are directly at odds with one another. The trend in Figure 10 suggests that the TES volume should be maximized in order to increase the overall gain of kWh produced, and Figure 11 suggests that the TES volume should be minimized in order to increase the overall efficiency of the precooling process. To balance these two parameters, the percent kWh gained over the extraction period and the percent kWh gained over the day were both normalized by their respective maximums and plotted versus the TES volume, as shown in Figure 12.

The trend in Figure 12 shows that the percent increase in kWh gained over the extraction period and the percent kWh gained over the day can be balanced out, and where they cross should determine the optimum TES volume, which is in this case is found to be about 2.55×10^7 channels in the PCM. Comparing the trend between change in TES volume and extraction time, obtaining the optimum TES volume also allows for the determination of the optimum extraction time.

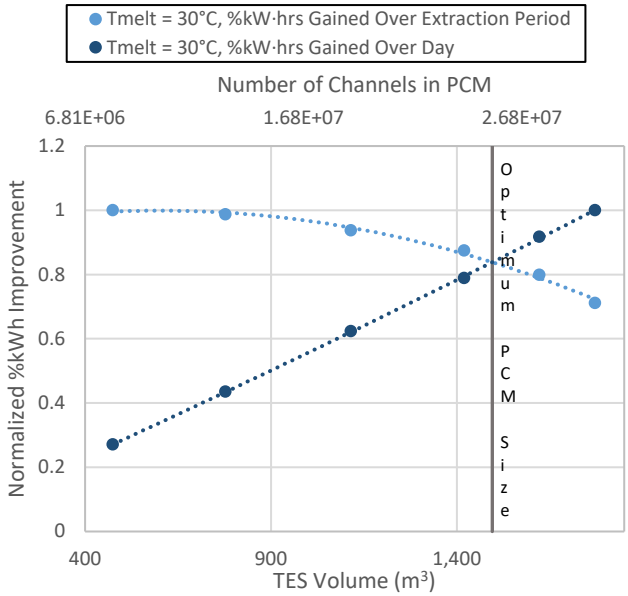

Fig. 12. %kWh gained over extraction period and %kWh gained over day both normalized by their respective maximums vs. TES volume for PCM melting temp. of T_m = 30°C in Las Vegas, NV for average day in August

Plotting TES volume versus the extraction time, as shown in Figure 13, with the provided parameters of a PCM melt temperature of 30°C and an average daily August temperature curve from Las Vegas, it was found that the optimum extraction time for the precooling process with these parameters was approximately 8.68 hours.

After adjusting the parameters of the TES volume and its corresponding extraction time within the model, the August temperature curve from Las Vegas was inputted into the model again, and the results are shown in Figure 14. Once again, it is observed that the melt fraction curve shows that the PCM is nearly fully melted and refrozen throughout the day. Figure 14 also shows that, during extraction, the precooling process

decreased the inlet air temperature to the steam condenser by about 6°C. This decrease in air temperature over the 8.68-hour extraction period increases the kWh produced during that time by 2.06% and increases the kWh produced throughout the entire day by 0.73%. These percentages correspond to a production gain of 9.0 MWh.

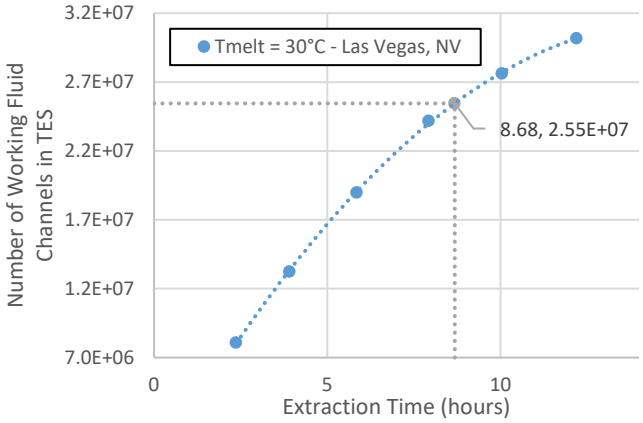

Fig. 13. Minimum required channels for 95% effectiveness (melting) vs. extraction time for PCM melting temperature of T_m = 30°C in Las Vegas, NV for average day in August

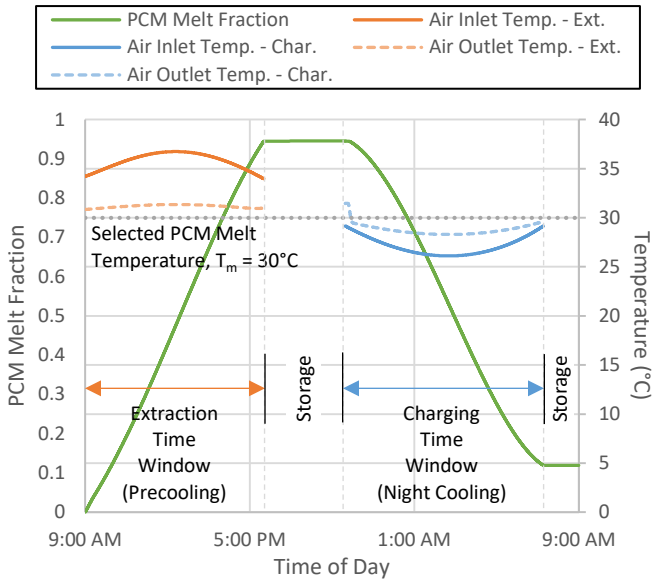

Fig. 14. Melt fraction of PCM and air inlet and outlet temperatures to and from TES for extraction (8.68 hours) and charging vs. time of day in Las Vegas, NV for average day in August

While the 2.06% gain of kWh over the extraction window is a significant increase in energy production during that time, the 0.73% gain of kWh over the day is desired to be increased further. To achieve this goal, different melt temperatures were explored. Figure 15 shows the trends between percent kWh gained over the extraction period versus the TES volume for three different PCM melt temperatures. These trends show that as the melt temperature is decreased, the same volume of the TES and same length of extraction can lead to greater amounts of kWh gained over the extraction period.

During the collection of this data, the model was once again adjusted to ensure that the PCM was being fully utilized throughout these extraction periods. To accomplish this full utilization, the number of channels in the PCM as well as the flow rate per channel in the PCM were attempted to be adjusted such that the extraction and charging processes would reach 95% effectiveness. However, it was found that as the melt temperature was pushed lower and lower, the charging process could no longer support a 95% effectiveness due to the minimum temperatures not achieving low enough values for a long enough time to substantially refreeze the PCM. It was therefore determined that simply lowering the PCM melt temperature would not be enough to increase the gain in kWh production; the minimum temperature achieved throughout the day would have to be adjusted as well.

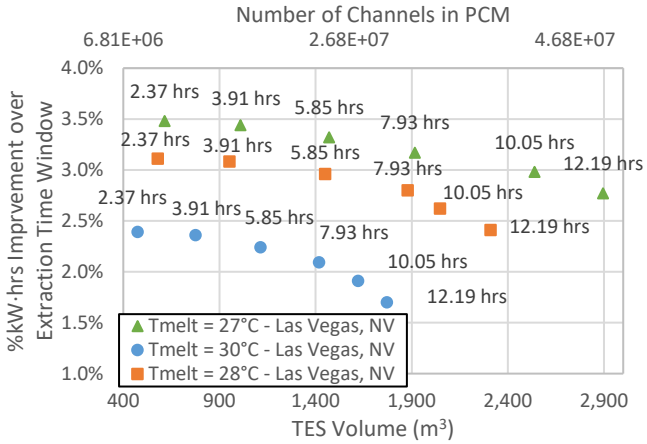

Fig. 15. %kWh gained over extraction time for different lengths of extraction periods vs. TES volume for various PCM melting temps. in Las Vegas, NV for average day in August

To push the minimum temperature achieved throughout the day to a lower value, different areas that are also in need of implementing water conservation techniques were considered. It was found that Reno, Nevada had slightly cooler, but comparable daytime temperatures to that of Las Vegas, but also had much cooler nighttime temperatures. With Reno as the new region of interest, weather data from January 2013 through December 2017 was obtained from the Reno Stead Airport Weather Station (WBAN 00279) through use of the Local Climatological Data Tool on the NOAA website [5]. The hourly temperature data from 2013 to 2017 for August is plotted in Figure 16. Looking at the average hourly temperatures over the years, it can be seen that August in Reno has a peak temperature of approximately 30°C and a low temperature of approximately 14°C. Looking back at Figure 5, it is observed that the low temperature in Reno for an average day in August is approximately 7°C cooler than the low temperature in Las Vegas for an average day in August.

Inputting the Reno average hourly temperatures for the month of August into the model, an approximate temperature

curve for an average 24-hour period in August was generated using a polynomial fit, as shown in Figure 17. Through temperature profile analysis, it was found that a PCM melt temperature as low as 21°C could support the desired charging effectiveness of 95%. With 21°C as the selected PCM melt temperature and using the temperature curve in Figure 17, it was determined that the extraction process could be implemented for a maximum of approximately 11 hours.

Using this 11-hour extraction time as a starting point, the model was again adjusted to contain a PCM that was large enough to be fully utilized throughout the entire extraction period, and the flow rate per channel in the PCM was adjusted such that the extraction and charging processes would both reach 95% effectiveness.

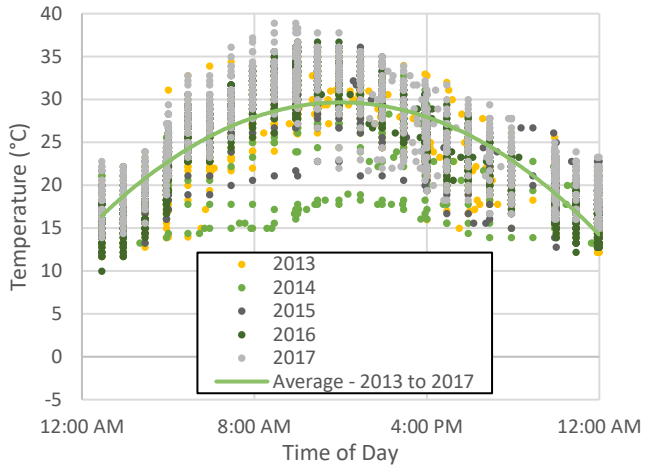

Fig. 16. Hourly temperature data for the month of August in Reno, NV for 2013 to 2017

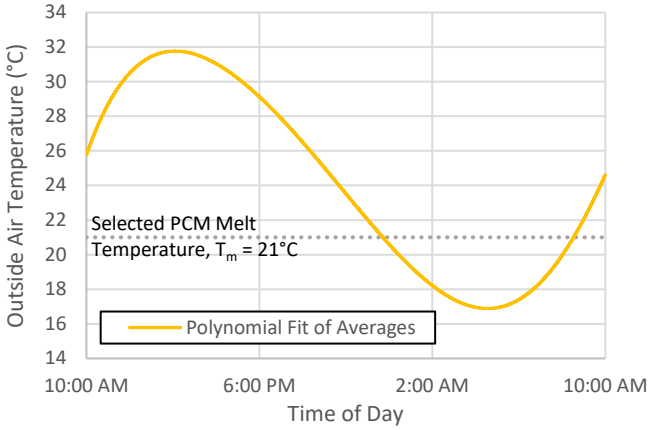

Fig. 17. Outside air temperature throughout an average August day in Reno, NV

After adjusting these parameters in the model, the Reno August temperature curve was inputted into the model. The results from using this ambient temperature data, the chosen PCM melt temperature, and the selected TES volume can be seen in Figure 18. In this figure, the melt fraction curve shows that the PCM was again nearly fully melted and refrozen throughout the day. Figure 18 also shows that during extraction, the precooling process with the selected parameters decreases the inlet air temperature into the steam condenser by about approximately 9°C, which is a great improvement over the Las Vegas result.

This decrease in air temperature over the 11-hour extraction period increases the kWh produced during that time by 2.97%, which is about 1.75 times greater of an increase than was seen with the non-optimized Las Vegas results. An increase of 1.36% of the kWh produced throughout the entire day was observed as well, which is about 1.6 times greater of an increase than was seen with the non-optimized Las Vegas results. These percentages correspond to a production gain of 17.2 MWh, which is about 1.65 times higher than the non-optimized production gain in kWh that was observed in the Las Vegas results.

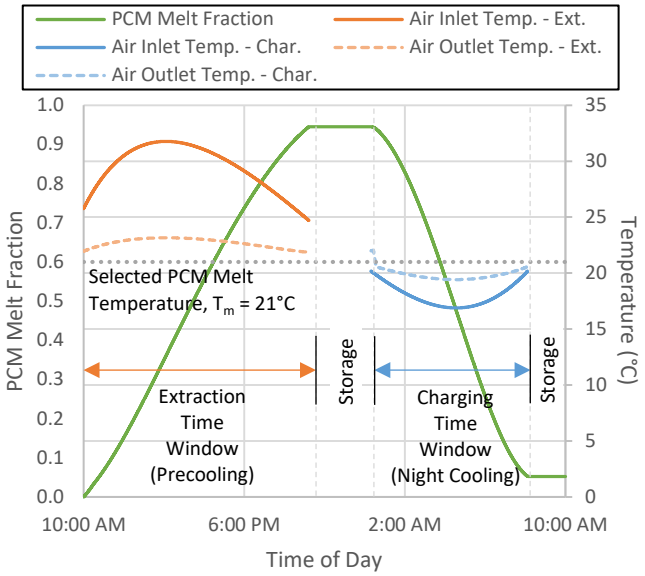

Fig. 18. Melt fraction of PCM and air inlet and outlet temperatures to and from TES for extraction (11 hours) and charging vs. time of day in Reno, NV for average day in August

Just as when analyzing the Las Vegas results, the goal of the precooling process is still to increase the efficiency of energy production by as wide a margin as possible. Again, several different extraction periods were tested to see if energy production could be further increased. To ensure that the PCM was being fully utilized throughout these extraction periods, the number of channels in the PCM as well as the flow rate per channel in the PCM were adjusted such that the extraction and charging processes would reach 95% effectiveness. Figure 19 shows the relationship between the percent increase in kWh over the extraction period and the volume of the TES.

Once again, a very clear relationship is observed in which the percent kWh gained over the extraction period increases as the volume of the TES, and therefore the length of extraction, increases. When comparing the Reno data to the Las Vegas data, it can also be seen that as the volume of the TES increases, the percent gain in kWh over the day from the Reno data increases

at a faster rate than that of the Las Vegas data, further demonstrating the effects of lowering the PCM melt temperature.

Figure 20 shows the relationship between the percent increase in kWh over the extraction period and the volume of the TES. As previously found, this data shows a relationship in which the percent kWh gained over the extraction period decreases as the volume of the TES, and therefore the length of extraction, increases. Comparing the Reno trend to the Las Vegas trend, it is observed that the Reno data, which corresponds to a lower PCM melt temperature, shows much better returns than that of the Las Vegas data, which corresponds to a higher PCM melt temperature.

Just as previously determined, the two relationships in Figures 19 and 20 have opposite trends from one another, and the percent kWh gained over the extraction period and the percent kWh gained over the day must both be normalized by their respective maximums in order to compare the two. Plotting the normalized data versus the TES volume, Figure 21 shows that the optimum TES volume for the given parameters is approximately 2.97×10^7 working fluid channels in the TES.

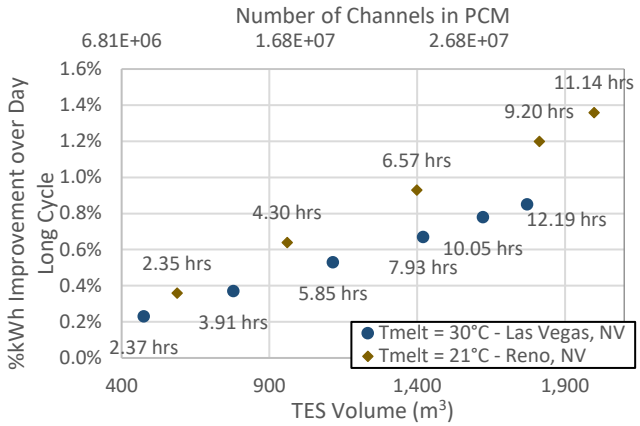

Fig. 19. %kWh gained over day for different lengths of extraction periods vs. TES volume for various PCM melting temps. in Las Vegas and Reno, NV for average day in August

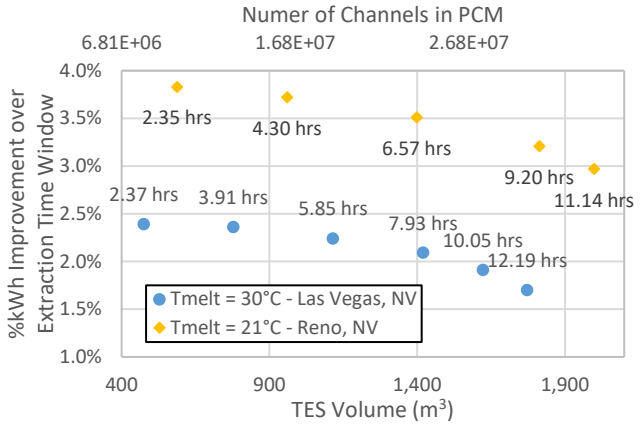

Fig. 20. %kWh gained over extraction time for different lengths of extraction periods vs. TES volume for various PCM melting temps. in Las Vegas and Reno, NV for average day in August

Once again, comparing the trend between change in TES volume and extraction time allows for the determination of the optimum extraction time. Plotting TES volume versus the extraction time, as shown in Figure 22, and with the provided parameters of a PCM melt temperature of 21°C and an average daily August temperature curve from Reno, it was found that the optimum extraction time for the precooling process with these parameters was approximately 8.94 hours.

After adjusting the parameters of the TES volume and its corresponding extraction time within the model, the August temperature curve from Reno was inputted into the model again, and the results are shown in Figure 23.

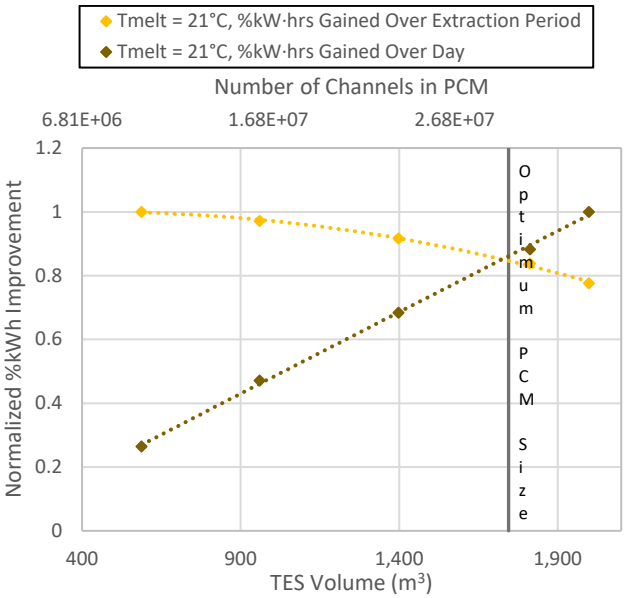

Fig. 21. %kWh gained over extraction period and %kWh gained over day both normalized by their respective maximums vs. TES volume for a PCM melting temp. of T_m = 21°C in Reno, NV for average day in August

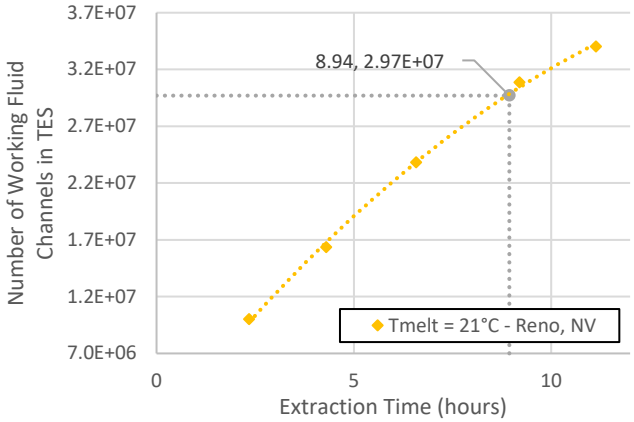

Fig. 22. Minimum required channels for 95% effectiveness (melting) vs. extraction time for a PCM melting temperature of T_m = 21°C in Reno, NV for average day in August

In these results, it is observed that the melt fraction curve displays the PCM nearly fully melting and refreezing throughout

the day. Figure 23 also shows that, during extraction, the precooling process decreased the air inlet temperature into the steam condenser by about 9°C. This decrease in air temperature over the 8.94-hour extraction period increases the kWh produced during that time by 3.25%, which is about 1.6 times greater of an increase than was seen with the optimized Las Vegas results. An increase of 1.18% of the kWh produced throughout the entire day was seen, which is about 1.6 times greater of an increase than was seen with the optimized Las Vegas results. These percentages correspond to a production gain of 14.9 MWh, which is about 1.43 times higher than the production gain in kWh that was observed with the optimized Las Vegas results.

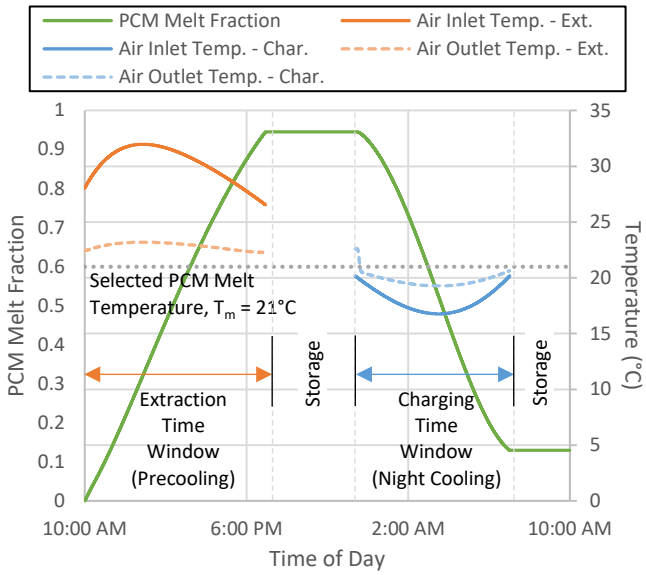

Fig. 23. Melt fraction of PCM and air inlet and outlet temperatures to and from TES for extraction (8.94 hours) and charging vs. time of day in Reno, NV for average day in August

Performing a cost analysis on the TES investment with optimized parameters, the savings achieved by the implementation of such a system as well as the amount of time it would take for the TES to pay for itself can be estimated. Project collaborators at Boeing have estimated the cost of the PCM and TES structure to be $15.19 per MJ of storage available within the PCM. Using the model to calculate the total storage provided by the PCM, it was found that for the optimized conditions, the Las Vegas PCM would have a capacity of 160,000 MJ of storage, and the Reno PCM would have a capacity of 171,000 MJ of storage. Using these values, it can be estimated that the initial capital investment of the TES in these cities would be $2.43 million and $2.60 million for Las Vegas and Reno, respectively.

For Las Vegas, the cost of the Southern Nevada Residential Single-Family program [6] is used to estimate the cost of electricity at $0.11 per kWh. Similarly, for Reno, the cost of the Northern Nevada Domestic Service program [7] is used to estimate the cost of electricity at $0.91 per kWh. Multiplying these pricing rates with the previously calculated optimized production gains in kWh per day for Las Vegas and Reno, it is calculated that the TES would provide revenue of $995 per day and $1,366 per day, respectively. Therefore, it would take approximately 23 years to pay back the initial capital investment of $2.43 million for the TES in Las Vegas and 18 years to pay off the initial capital investment of $2.60 million for the TES in Reno. This payback time estimation assumes that the TES is in use daily with consistent efficiency during the summer months of June through September, expects all of the excess profit resulting from the implementation of the TES system is used as the only source of payment, and accounts for continuously compounding interest at a rate of 10%. There would, of course, also be additional costs associated with heat exchanger and pump investments that would be required to support the TES system. It is also noted that the electricity cost estimations here have been limited to residential applications; however, similar estimations have been performed for commercial applications, and comparable conclusions have been reached.

CONCLUSION

The goal of this study was to use Helmns and Carey's model of TES in conjunction with a subsystem that utilizes cool storage to precool the air flow for a power plant air-cooled condenser during peak daytime air temperatures. This model was used to explore the parametric effects of changing PCM melt temperature and the energy storage and extraction control settings for the system. The subsystem model was also computationally linked to a model of Rankine cycle power plant performance to predict how much additional power the plant could generate as a result of the asynchronous cooling augmentation provided by this subsystem.

With this multi-scale modeling, the performance of the TES unit was examined within the context of a larger subsystem to illustrate how a high efficiency, optimized design target could be established for specified operating conditions. By adjusting the flow rate within the fluid flow passages and the volume of the TES to achieve complete melting of the PCM during a set extraction time, the percent increases in kWh over the extraction period and over a 24-hour period were calculated for various extraction times. The percentage increase in kWh over the extraction period ranged from 1.75% to 3.75%, and the percentage increase in kWh over a 24-hour period ranged from 0.25% to 1.35%. Variances in these percentages depended on location, daytime high and nighttime low temperatures, and length of the extraction period.

Peak power output enhancements were observed to occur when the system operated in the extraction phase during limited hours near the peak temperatures experienced throughout a day, while total kWh enhancements were shown to increase as the extraction period increased. For example, looking at the Reno model, the maximum kWh increase over an extraction period was calculated to be about 3.75% and was observed to occur over an extraction length of about 2.35 hours, where temperatures were approximately 10°C above the melting temperature of the PCM. The maximum kWh increase over a 24-period was calculated to be about 1.35% and was observed to occur over an

extraction length of 11.14 hours, where temperatures fluctuated from approximately 1 to 10°C above the PCM melt temperature.

Obtaining the optimal amount of PCM for both the percent kWh increase over the extraction period and the percent kWh increase over a day, the results suggest that for a full-sized power plant with a nominal capacity of 50 MW, the kWh output of the plant can be increased by up to 3.25% during the heat input/cold extraction period and up to 1.18% over a 24-hour period, depending on parameter choices. For these optimized conditions, cost analyses were performed, and it was estimated that the TES system has the potential to provide additional revenue of up to $995 per day and $1,366 per day, respectively, for Las Vegas and Reno. With initial investments for the PCM and TES structures adding up to $2.43 million in Las Vegas and $2.60 million in Reno, the payback periods were estimated to be 23 years and 18 years, respectively.

Results obtained to date are not fully optimized, and the results suggest that with further adjustments in system parameters, weather data input, and control strategies, the predicted enhancement of the power output can be increased above the results in the initial performance predictions reported here.

ACKNOWLEDGEMENTS

Support for this research was provided by the ARID program of ARPA-E. Research assistance from the Energy and Multiphase Transport Laboratory at UC Berkeley is also gratefully acknowledged.

REFERENCES

[1] M. M. Alkilani, K. Sopian, S. Mat and M. A. Alghoul, "Output Air Temperature Prediction in a Solar Air Heater Integrated with Phase Change Material," *European Journal of Scientific Research*, vol. 27, no. 3, pp. 334-341, 2009.

[2] S. M. Vakilaltojjar and W. Saman, "Analysis and modelling of a phase change storage system," *Applied Thermal Engineering*, vol. 21, no. 3, pp. 249-263, 2001.

[3] A. Helmns and V. P. Carey, "Multi-Scale Transient Modeling of Latent Energy Storage for Asynchronous Cooling," *Journal of Thermal Science and Engineering Applications*, 2018.

[4] "The Other Foot Print," *EPRI Journal*, no. 2, p. 11, 2010.

[5] "Data Tools: Local Climatological Data (LCD)," NOAA National Centers for Environmental Information, [Online]. Available: https://www.ncdc.noaa.gov/cdo-web/datatools/lcd. [Accessed November 2017].

[6] Nevada Power Company, "NV Energy Electric Rate Schedules for Residential Customers," 1 April 2018. [Online]. Available: https://www.nvenergy.com/publish/content/dam/nvenergy/brochures_arch/about-nvenergy/rates-regulatory/np_res_rate.pdf. [Accessed April 2017].

[7] Sierra Pacific Power Company, "NV Energy Electric Rate Schedules for Residential Customers," 1 April 2018. [Online]. Available: https://www.nvenergy.com/publish/content/dam/nvenergy/brochures_arch/about-nvenergy/rates-regulatory/spp_nv_resrates.pdf. [Accessed April 2018].